

KOHIO, HINISSAN PASCALINE, M.S. Glycolytic Control of Vacuolar ATPase Pump Activity: A Mechanism to Regulate Influenza Viral Infection. (2012)
Directed by Dr. Amy Adamson. 43 pp.

Influenza viruses are pathogens that can cause major pandemics in the human population, such as the Spanish Flu outbreak in 1918-1919, which caused about 50 million deaths worldwide. As the virus frequently mutates, vaccines and anti-viral drugs can be rendered ineffective over time. As new influenza viruses emerge, new anti-viral therapies are essential. The goal of this study was to identify novel means to inhibit influenza viral replication, by targeting the activity of the Vacuolar ATPase (V-ATPase) proton pump. The V-ATPase pump is a multi-molecular proton pump that couples ATP hydrolysis to proton transport, thus regulating the pH of intracellular compartments. This activity is also used by the influenza virus to induce viral uncoating during infection. In this study, I examined how changes in glucose concentrations affect V-ATPase pump activity and influenza replication. Through immunostaining of mammalian cells, I observed that higher levels of glucose caused specific localization of the V-ATPase proton pumps within the cell, thus triggering pump activity. Western blot analysis of two V-ATPase proton pump proteins showed that protein synthesis of the pump was not affected by increasing the amount of glucose. Based on these results, I examined the effect of increasing glucose levels upon influenza infection. I found that higher amounts of glucose yielded higher influenza infection levels. Additionally, viral infection was significantly reduced after inhibition of glycolysis with 2-deoxyglucose and 3-bromopyruvate. Lastly, I bypassed the need for glycolysis via addition of extracellular ATP. The V-ATPase pump activity was restored after glycolytic inhibition with ATP

treatment as indicated by an increased number of virally infected cells. Taken together, I propose that inhibiting influenza replication in mammalian cell cultures by altering activity of the V-ATPase proton pump via inhibition of glycolysis could be a potential new approach for the treatment of influenza infection.

GLYCOLYTIC CONTROL OF VACUOLAR ATPASE PUMP ACTIVITY: A
MECHANISM TO REGULATE INFLUENZA VIRAL INFECTION

By

Hinissan Pascaline Kohio

A Thesis Submitted to
the Faculty of the Graduate School at
The University of North Carolina at Greensboro
in Partial Fulfillment
of the Requirements for the Degree
Master of Science

Greensboro
2012

Approved by

Committee Chair

To my parents and family for their unconditional love and support.

APPROVAL PAGE

This thesis has been approved by the following committee of the Faculty of the Graduate School at the University of North Carolina at Greensboro.

Committee Chair _____

Committee Members _____

Date of Acceptance by Committee

Date of Final Oral Examination

ACKNOWLEDGEMENTS

I would like to thank my advisor and committee chair Dr. Amy Adamson for all the support, time and energy she has contributed during my graduate research experience. This thesis would not have been a success without her guidance and encouragement.

I would like to thank my committee members Dr. John Tomkiel and Dr. Yashomati Patel for their time and suggestions that made this project successful.

Lastly, I would like to thank my family for their constant support and encouragement through my educational experience.

TABLE OF CONTENTS

	Page
LIST OF FIGURES	vi
CHAPTER	
I. INTRODUCTION	1
Influenza Virus.....	1
Vacuolar ATPase Proton Pump	5
Glycolysis and Vacuolar ATPase	8
Project Overview	11
Specific Aims.....	11
II. MATERIALS AND METHODS.....	12
Reagents.....	12
Cell Culture.....	12
Infection Medium.....	12
Immunostaining for V ₁ A ₁ and V ₁ B _{1/2}	13
Immunostaining for HA.....	14
Western Blot for V ₁ A ₁ and V ₁ B _{1/2}	14
Immunostaining for HA after 2-DG, 3-BrPa, LND and 6-AN Treatment	15
Immunostaining for HA after ATP Treatment.....	15
Data Analysis	16
III. RESULTS	17
The effect of glucose at low and high concentrations on V-ATPase pump localization/assembly	17
Influenza viral infection is altered in response to changes in glucose concentration.....	20
Increased glucose does not increase pump protein expression levels	24
Inhibiting early glycolysis inhibits influenza viral infection	27
IV. DISCUSSION.....	36
REFERENCES	41

LIST OF FIGURES

	Page
Figure 1. Schematic representation of influenza virus.....	2
Figure 2. Influenza replication.....	3
Figure 3. V-ATPase pump structure.....	7
Figure 4. Pathway of glycolysis.....	10
Figure 5. V-ATPase pump localization/assembly at low and high glucose concentration.....	19
Figure 6. Increasing amounts of glucose increase influenza viral infection of MDCK cells.....	22
Figure 7. Graphical representation of the percentage of infected cells.....	23
Figure 8. V-ATPase protein synthesis is not affected at varying glucose conditions.....	25
Figure 9. V-ATPase protein levels.....	26
Figure 10. Confocal imaging of glycolytic pathway inhibition on influenza viral infection.....	29
Figure 11. Percentage of infected cells after glycolytic inhibition.....	30
Figure 12. Effect of the addition of extracellular ATP.....	32
Figure 13. Percentage of infected cells after addition of extracellular ATP.....	33
Figure 14. Percentage of infected cells after inhibition of the pentose phosphate pathway.....	35
Figure 15. Schematic representation of glucose metabolism on V-ATPase activation and influenza viral infection.....	40

CHAPTER I
INTRODUCTION

Influenza Virus

Influenza viruses are respiratory viruses, and members of the *orthomyxovirus* family. Influenza viruses are single-stranded negative RNA viruses with eight RNA molecules found within an envelope. Four of the RNA segments code for specific ribonucleoproteins (RNPs): the PB1, PB2, PA polymerase proteins and the nucleoprotein (NP). The other four RNA segments code for essential proteins: the glycoproteins hemagglutinin (HA) and neuraminidase (NA), the ion channel or integral protein (M2), and the matrix protein (M1) which is thought to be required during viral assembly and recruitment at the apical membrane (Palese and Shaw 2007). The nuclear export protein (NEP) and the nonstructural protein 2 (NS2) are suggested to play a role in RNP export during budding (Figure 1) (Palese and Shaw 2007). It is important to note that some of the RNA segments code for two proteins. The lipid envelope of the virus is derived from the host plasma membrane and harbors the two glycoproteins HA and NA and the ion channel M2 (Palese and Shaw 2007). Three types of influenza viruses which are antigenically different have been identified: influenza A, B, and C.

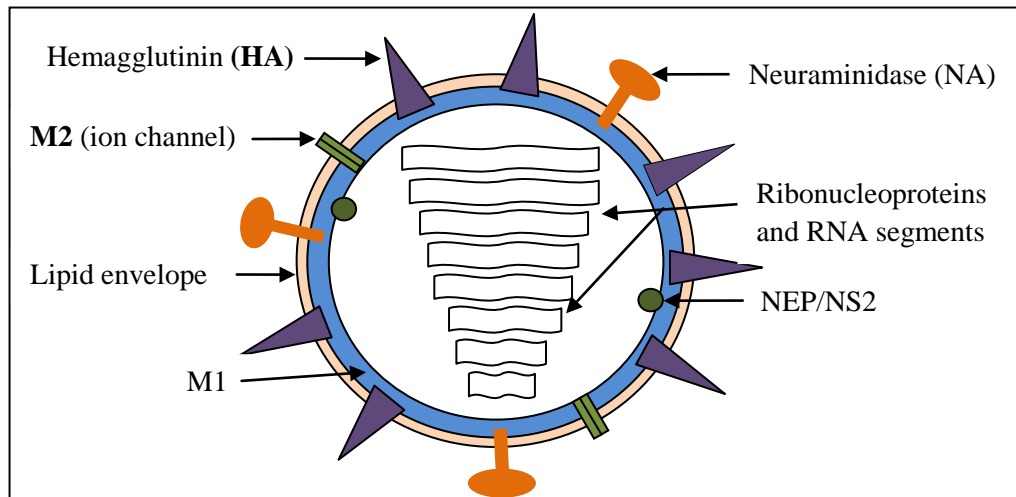


Figure 1. Schematic representation of influenza virus. The RNA polymerases, the nucleoprotein (NP) and all RNA segments are located in the interior of the envelope. (Modified from Palese and Shaw 2007).

Influenza can infect a wide range of organisms from mammals to birds, causing major pandemics as well as endemics and epidemics. One significant outbreak was identified in 1918 and is commonly referred to as the “Spanish flu”. This led to at least 50 million deaths worldwide in 1918-1919 (Betakova 2007). Other pandemics were identified in 1957, 1968, 1977 and 2009 (Palese and Shaw 2007, CDC), mostly caused by an influenza type A virus.

Influenza viruses lead to severe infection of the epithelial cells of the upper and lower respiratory tract. Infection by the influenza virus is caused by the transport of viral genome into the nucleus of the host cell where transcription and replication of the viral genome take place (Palese and Shaw 2007, Betakova 2007) (Figure 2).

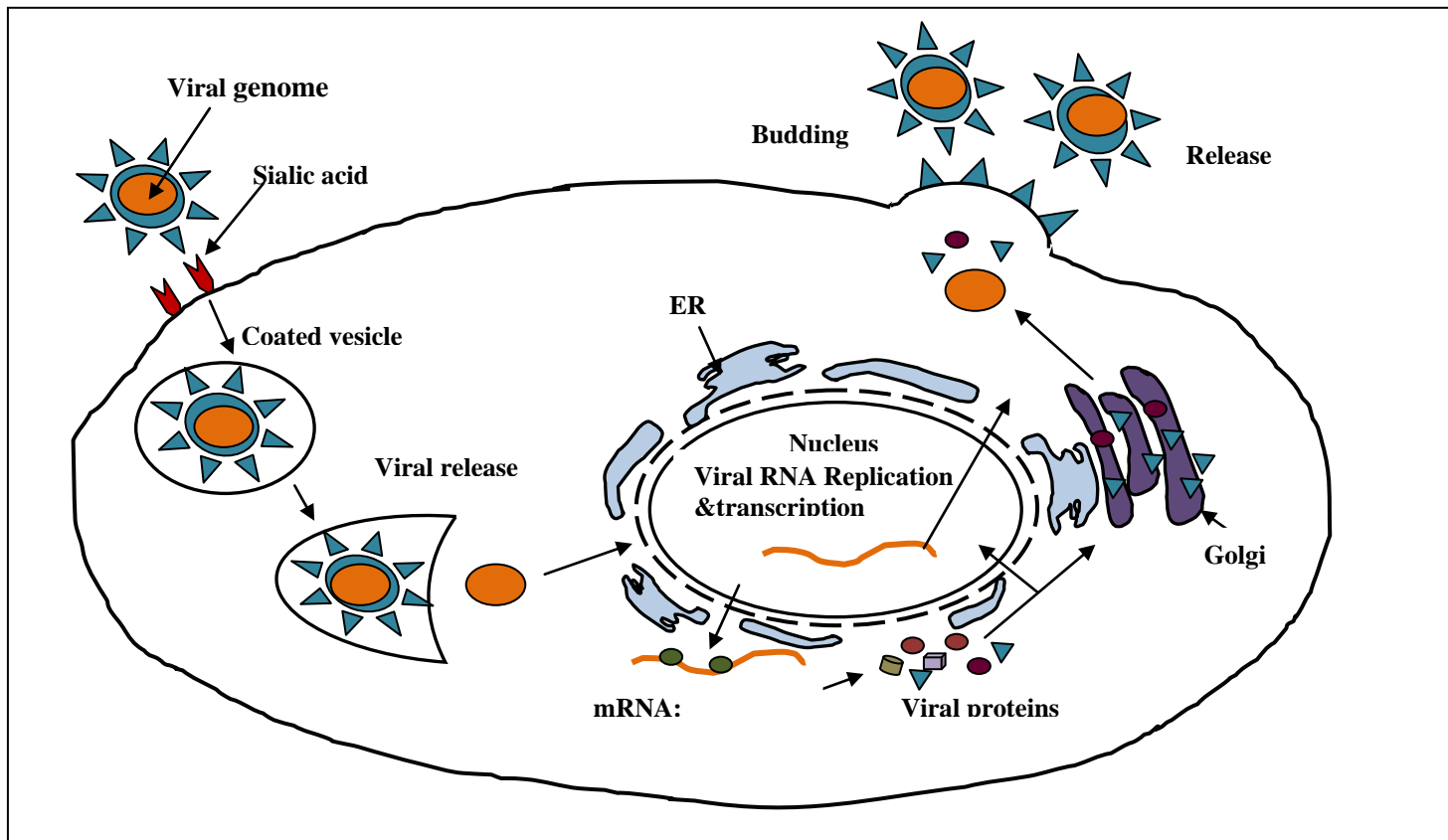


Figure 2. Influenza replication. After endocytosis by binding to sialic acid (receptor), the viral genome is released into the cytoplasm and transported into the nucleus. Replication and transcription of the viral genome take place in the nucleus. The mRNA is transported to the cytoplasm where translation of viral proteins takes place. Polymerases, NP, and NS₂ are transported back into the nucleus to further aid viral replication. Viral assembly occurs at the plasma membrane. HA, NA, and M2 glycoproteins are sent to the plasma membrane via the Golgi apparatus. (Modified from Influenza Report 2006).

Entry of the virus into the cytoplasm is initiated by binding of the HA glycoprotein to its receptor sialic acid on the cell surface. Following attachment, the virus is transported into the cytoplasm in an endocytic vesicle. The M2 ion channel plays a significant role in viral uncoating. In fact, the M2 protein, which is activated by the acidic pH of the vesicle (Pinto and Lamb 2006, Betakova 2007), transports protons from the vesicle into the interior of the virion. M2 activity helps lower the pH inside the virion, allowing viral uncoating through dissociation of M1 from the viral genome (Betakova 2007). In addition, the decrease in pH also helps release the viral genome by promoting a conformational change in the HA glycoprotein which triggers the fusion of the endosomal membrane with that of the viral membrane (Palese and Shaw 2007).

Following replication using its own polymerases (within the nucleus), the virus is assembled at the apical membrane of the cell where the new viral particles bud and release into the cytoplasm (Palese and Shaw 2007). Release of viral particles is initiated by NA activity that cleaves sialic acid from the cell surface. This activity allows dissociation of the virus from the cell (Betakova 2007).

Influenza viruses can undergo reassortment, where different RNA segments are selected from cells infected with multiple influenza viruses (Palese and Shaw 2007). Reassortment leads to the emergence of new potentially infectious strains. In fact, the 1957 and 1968 pandemics emerged as a result of the reassortment of viral genomes (Palese and Shaw 2007).

Antiviral drugs have been used for the treatment of influenza infection. Amantadine and rimantadine are two inhibitors of the M2 protein that are mostly

effective in the treatment of influenza type A (Palese and Shaw 2007). These drugs act by blocking M2-mediated proton transport into the virion. Zanamivir and oseltamivir are effective on both influenza type A and B (Palese and Shaw 2007). They act by inhibiting the NA glycoprotein. However, the virus develops a rapid resistance to the drugs which limit their effectiveness (Betakova 2007). In addition to the drug treatment, influenza vaccines have been used. Unfortunately, the vaccines may not be fully effective since they are based on the previous influenza strains which may not emerge at a given time. The M2 ion channel is essential for viral uncoating through acidification of the interior of the viron. However, one additional protein complex, the Vacuolar H⁺ ATPase proton pump located within endosomal membranes, was also identified to be involved in influenza viral entry by maintaining the acidic pH necessary for viral release (Guinea et al 1995, Jefferies et al 2008).

Vacuolar ATPase Proton Pump

Vacuolar type H⁺ ATPases (V-ATPases) are multisubunit proton pumps that couple ATP hydrolysis to the transport of protons from the cytoplasm into the lumen of endosomes or organelles. This activity leads to the acidification of intracellular compartments, necessary for multiple cellular processes (Jefferies et al 2008). V-ATPase pumps share similar function and structure with the F-ATPase pumps found in the plasma membrane of bacteria (Nishi & Forgac 2002).

The V-ATPase pumps were first identified in lysosomal compartments and the central vacuole of the yeast *Saccharomyces cerevisiae* and in plants (Kakinuma et al.

1981), necessary for macromolecule degradation. V-ATPase pumps are now known to be ubiquitously found in the endomembrane system of eukaryotic cells including mammalian cells. The V-ATPase pumps were also found to be present in the collecting duct of mammalian kidney (Wagner et al. 2004), osteoclasts (Chatterjee et al. 1992), sperm, macrophages, and insect gastrointestinal epithelia (Harvey, W.R 1992 and Klein 1992). Therefore, V-ATPase pumps exist on the plasma membranes of specialized cells and within many organelles.

V-ATPases are composed of a peripheral V_1 domain (400-600 kDa) and an integral V_0 subcomplex (150-350 kDa) (Figure 3). The V_1 subcomplex contains eight subunits, two of which interact with ATP and provide the energy necessary for active transport of protons against a concentration gradient. Subunits of the V_1 domain are represented by the capital letters A, B, C, D, E, F, G, and H. The V_0 subcomplex which consists of six subunits carries proton transport into the lumen. Subunits of the V_0 domain are identified by the lower case letters a, c, d and e, with subunit c consisting of different isoforms, c' and c'' (Jefferies et al. 2008). The V_1 and V_0 domains form two ring structures that function through a rotary mechanism (Hirata et al. 2003). ATP binding to the catalytic sites on the V_1 domain, specifically on the A and B subunits, leads to conformational changes in the A subunit which drives rotation of the rotor comprised of subunits D, F and d and the proteolipid c-ring (Jefferies et al. 2008 and Beyenbach et al. 2006). This activity drives proton translocation from the cytoplasm into the lumen through passage via the V_0 a subunit (Figure 3).

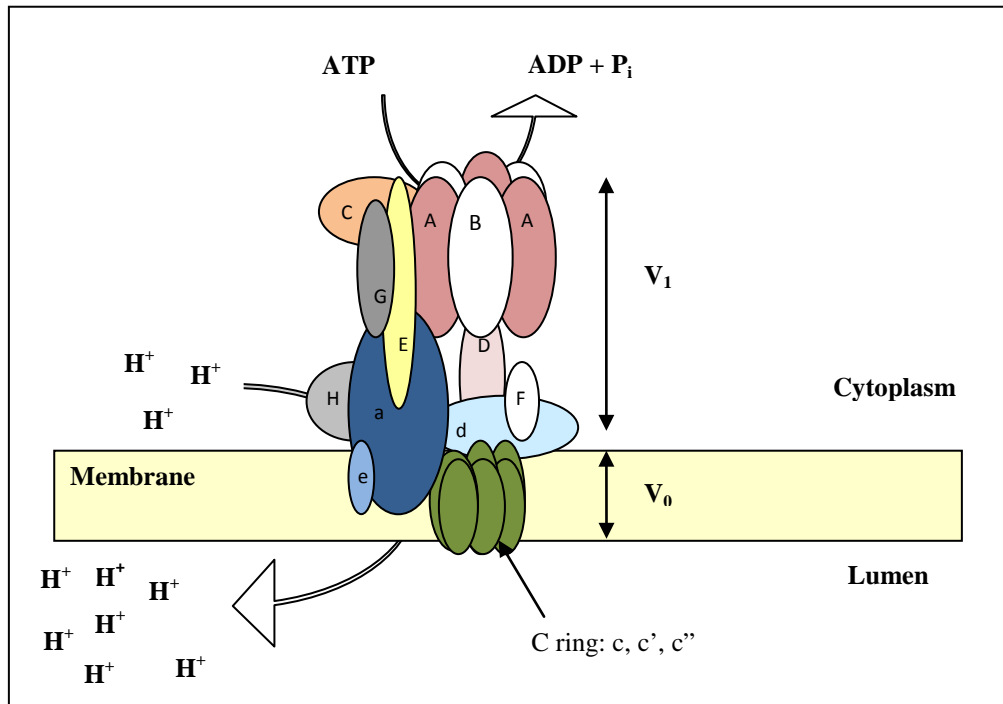


Figure 3. V-ATPase pump structure (Modified from Sze, 2002 and Kane, 2006).

V-ATPase activity is regulated through disassembly of the V₁ and V₀ domains. This process helps regulate the pH levels of organelles inside the cell (Bond and Forgac 2008). One of the mechanisms that regulate the V-ATPase activity is glucose depletion (Kane 2006). A V-ATPase dissociation mechanism was first observed in yeast and *Manduca sexta* (Kane, 2006). It has also been shown to take place in mammals and insects (Xu and Forgac 2001). During disassembly, the C subunit of the V₁ domain is released, which suggests its role in the pump assembly and disassembly (Beyenbach and Wiczoreck 2005, Jefferies et al 2008). V-ATPase assembly and disassembly induced by glucose levels is independent of the main glucose repression/depression pathway or Ras-cAMP pathway as well as other signal transduction pathways (Parra & Kane 1998). In

fact, glycolysis has an indirect effect on V-ATPase activity. Pump disassembly can also result from a reduction in ATP levels (Para and Kane 1998).

Glycolysis and Vacuolar ATPase

The Embden - Myerhof pathway, commonly referred to as glycolysis, is the process by which glucose metabolism occurs to generate a net gain of two ATP, two molecules of NADH^+ and two molecules of pyruvate at the end of glycolysis (Pelicano et al. 2006). Glycolysis takes place in two major phases. The primary phase involves the combustion of two ATP to convert glucose into fructose 1-6-bisphosphate. The second stage of glycolysis converts fructose 1-6-bisphosphate into molecules of glyceraldehyde - 3-phosphate (GAP) and dihydroxyacetone phosphate (DHAP) that is further oxidized into lactate or pyruvate. DHAP is converted back into GAP before further oxidation. Specific enzymes catalyze each stage of glucose metabolism (Figure 4) (Pelicano et al. 2006).

Glycolysis has an indirect effect on V-ATPase activity; however there is a lack of understanding on how the energy from ATP hydrolysis is provided to the V-ATPase pumps needed for proton transport into the lumen (Lu et al. 2004). Studies on yeast and mammals indicate a direct physical interaction between V-ATPases and aldolase, one of the glycolytic enzymes that converts fructose-6-phosphate into GAP (Lu et al. 2001). There is an increase in physical interaction between aldolase and the α , β and ϵ subunits of V-ATPases pumps when glucose is present (Lu et al. 2004). Furthermore, disassembly and reduced levels of V-ATPase activity were observed in mutant aldolase yeast cells, and normal pump assembly and activity was restored after introduction of the wild-type

aldolase gene into the mutant cells (Lu et al. 2004). These findings provide evidence that the glycolytic enzyme aldolase mediates V-ATPase assembly and activity (Lu et al. 2004). V-ATPase and aldolase physically interact, and in human kidney cells the rate limiting enzyme of glycolytic pathway, phosphofructose kinase 1 (PFK-1) interacts with the α -subunit of the pump via the C-terminus region of the subunit (Su et al. 2003). A study conducted in our lab also identified glyceraldehyde-3 phosphate dehydrogenase (GAPDH) as a modifier of M2 ion channel activity (Unpublished). Thus alterations in glycolysis may affect V-ATPase activity, and this in turn may affect M2 activity, and therefore alter influenza replication.

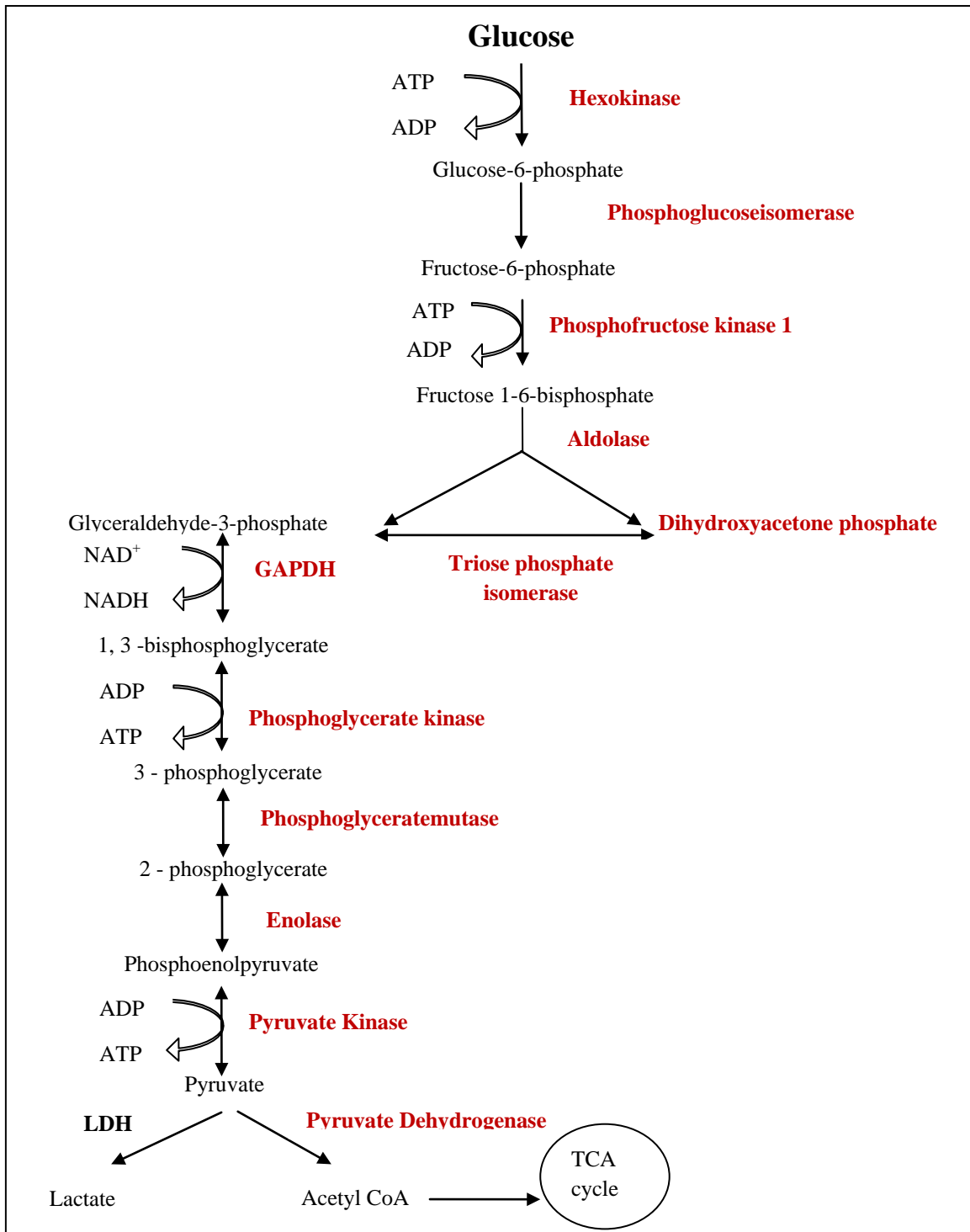


Figure 4. Pathway of glycolysis. All glycolytic enzymes are represented in red. Glyceraldehyde-3 phosphate dehydrogenase (GAPDH), lactate dehydrogenase (LDH) (Modified from Pelicano et al., 2006).

Project Overview

The primary function of the V-ATPase proton pump is to acidify intracellular compartments. The lowered endosomal pH sustained by V-ATPase pumps also plays a crucial role in influenza viral infection. Influenza virus enters the host cell through endocytosis and is contained within a vesicle. The viral genome is released in response to the low pH provided by the V-ATPase pumps found in the vesicle, via an increase in M2 activity. The goal of this study was to address the implication of V-ATPase pumps activity with respect to glucose metabolism, and how this process affects influenza viral infection of mammalian cells.

Specific Aims

1. Analyze the effect of glucose at low and high concentrations on V-ATPase pump localization/assembly.
2. Investigate if influenza infection is dependent upon glucose levels.
3. Determine if changes in glucose concentrations affect the protein expression levels of the V-ATPase pump components.
4. Determine the effect of glucose metabolism in influenza viral infection.

CHAPTER II

MATERIALS AND METHODS

Reagents

2-deoxyglucose (2-DG) (Product # D8375), 3-bromopyruvate (3-BrPa) (Product # 16490), Lonidamine (LND) (Product # L4900), 6-aminocicotinamide (6-AN) (Product # A68203) and Adenosine 5' trisphosphate disodium salt hydrate (ATP) (Product # A2383) were purchased from Sigma. Cells and influenza A H1N1 virus (A/PR/8/34) (Product # VR-1469) were purchased from ATCC.

Cell Culture

Human cervical cancer (HeLa) and Madin-Darby Canine Kidney (MDCK) cells were maintained in a high glucose Dulbecco's Modified Eagles Medium (DMEM) from Thermo Scientific supplemented with 10% Fetal Bovine Serum (FBS) as well as penicillin/streptomycin (500 μ l) and an antifungal agent (500 μ l). Cells were maintained at 37°C in an air jacketed incubator with 5% CO₂.

Infection Medium

Infection medium was prepared using influenza A H1N1 virus (A/PR/8/34) at a Multiplicity of Infection (MOI) of 1, contained in low glucose DMEM from Thermo Scientific along with 1 μ g/ml trypsin, 0.125% BSA, and 1% HEPES. No serum, penicillin

nor antifungal agent were added. Cells were treated accordingly for 24 hr with 2ml of the infection medium containing influenza A virus.

Immunostaining for V₁A₁ and V₁B_{1/2}

Confluent HeLa cells were plated (8×10^4 cells/ml) on coverslips in 35 mm cell culture dishes each containing 1mg/ml (low) for our control treatment and 6mg/ml (high) glucose (total volume of 2ml of medium was added to each plate). Twenty-four hour later, 1 μ l of Fu-gene (Transfection reagent) (Promega) was added to each plate. Cells were washed with 1x phosphate buffered saline (PBS) and a fresh glucose-containing media was added for another 24 hr. Coverslips were transferred to a 24 well plate, rinsed in 1xPBS and fixed in 4% paraformaldehyde at room temperature for 15min. Cells were incubated in incubation mix (1xPBS, 0.3% BSA, 0.1% Triton X, 5% goat serum) for 10 min. Cells were incubated for an additional 1hr at 37°C with V₁A₁ (Product # sc-20943) or V₁B_{1/2} (Product # sc-28801) (Santa Cruz) primary antibody, diluted 1:200 in incubation mix. Cells were washed 4 times with 1xPBS on a rotating platform followed by incubation for another 40 minutes at 37°C with a Donkey-Anti-Rabbit -CY3 (Jackson ImmunoResearch Laboratories) secondary antibody diluted 1:200. Cells were washed 4 times as previously described. Hoescht stain was diluted 1:2000 in 1xPBS for the last wash. Coverslips were mounted in Fluorescent Mounting Medium (DakoCytomation).

Immunostaining for HA

Confluent MDCK cells were harvested then plated at (8×10^4 cells/ml) in 2ml of low glucose and allowed to grow for 24 hr in 35mm cell culture dishes with coverslips. Cells were plated at 1(control), 2, 3, 4, 5 or 6mg/ml of. After 24 hr, cells were washed with 1x PBS, infected with influenza A H1N1 and new glucose was added. Cells were infected for 24hr. Immunostaining was conducted as previously. An anti -HA primary antibody (Product # sc-52025) (Santa Cruz) with a dilution of 1:200 was used. A Goat-Anti-Rabbit -CY3 (Jackson ImmunoResearch Laboratories) secondary antibody was diluted 1:400.

Western Blot for V₁A₁ and V₁B_{1/2}

HeLa cells were plated (8×10^4 cells/ml) in 2 ml media containing at 1(control), 2, 3, 4, 5 or 6mg/ml of glucose. Twenty-four hour later, 1 μ l of Fu-gene (Promega) was added. Cells were washed with 1x PBS and a fresh glucose-containing media was added for another 24 hr. Cells were suspended in 1xPBS and the pellets were lysed in 8M urea. Cells were mixed with equal volume of 2x protein loading dye. Western blotting was performed to separate the protein on a 10% SDS- polyacrylamide electrophoresis gel using a Bio-Rad Mini-Protean gel apparatus. Gel was run at 200 volts for 30min in 1x running buffer. The proteins were transferred to a nitrocellulose membrane in a 1x electroblotting buffer. The blot was then blocked in a 1xPBS, 0.1% Tween 20 (Fisher Scientific) and 5% bovine serum albumin (BSA) (Fisher Scientific) solution. The membrane was incubated in a 1:2000 dilution of anti- V₁A₁ or V₁B_{1/2} (Santa Cruz)

primary antibody for 1 hr at room temperature or overnight at 4 °C, and washed with 1xPBS, 0.1% Tween 20. The membrane was incubated with GAM-HRP (Goat-Anti-Mouse-Horseradish Peroxidase) secondary antibody from Jackson ImmunoResearch Laboratories, diluted 1:10,000 in blocking solution with gentle rocking at room temperature for 30-60 min. The membrane was washed, and bound antibody visualized using SuperSignal (Thermo Scientific Pierce). BioRad gel documentation was used to acquire image chemiluminescence and bands were quantified using Quantity 1 software.

Immunostaining for HA after 2-DG, 3-BrPa, LND and 6-AN Treatment

MDCK cells were plated in 4.5mg/ml of glucose (DMEM) from Thermo Scientific. Cells were treated 24 hr later with 2-DG (0, 0.25, 2, 5mM), 3-BrPa (0, 30, 300, 600 μ M) or LND (0, 6, 62.5, 200 μ M,) (concentrations were established from Hulleman E. et al. (2008)), or 6-AN (0, 30, 140, 250 μ M) (concentrations established from Budihardjo I. et al. (1998)). Cells were infected with influenza A H1N1 for 24 hr following treatment with the drugs. 24 hr post infection, cells were washed with 1xPBS and new medium was added without the drugs. Immunostaining was conducted following the same procedure as immunostaining for V₁A₁ and V₁B_{1/2}, instead using an anti-HA primary antibody diluted 1:200 and a Goat-Anti-Mouse-CY3 secondary antibody diluted 1:400.

Immunostaining for HA after ATP Treatment

MDCK cells were plated in 4.5mg/ml glucose (DMEM) from Thermo Scientific. Cells were treated 24 hr later with 2-DG (5mM). Cells were subsequently treated with

ATP (50, 100 μ M) (concentrations established from Probst I. et al. (1989)), along with influenza A H1N1. ATP treatment and influenza infection was conducted for 24hr. Cells were fixed and stained with an anti-HA primary antibody and a Goat-Anti-Mouse-CY3 secondary antibody as previously described.

Data Analysis

Images of immunostained cells were captured on Olympus Fluoview FV 500/IX 81confocal microscope. Bound antibodies for Western Blot analysis were viewed using a BioRad imager and quantified using Quantity 1 software. Data were statistically analyzed using the student T-test.

CHAPTER III

RESULTS

The effect of glucose at low and high concentrations on V-ATPase pump localization/assembly

V-ATPase pump activity is downregulated by glucose depletion through disassembly of the peripheral V_1 and the integral V_0 domain in yeast *Saccharomyces cerevisiae* cells (Para and Kane 1995). Additionally, pump assembly is modulated by the relative concentration of extracellular glucose in yeast (Kane 1995). I further analyzed pump assembly at low and high glucose concentrations in mammalian cells to visualize the pump's localization and assembly within mammalian cells. To examine the V-ATPase pump's localization/assembly, HeLa cells lines were grown at 1mg/ml (low) or 6mg/ml (high) glucose. Cells were then immunostained with anti- V_1A_1 and $V_1B_{1/2}$ primary antibodies and visualized using confocal microscopy. Images of cells showing the pumps localization/assembly are shown in Figure 5. The use of both anti- V_1A_1 and $V_1B_{1/2}$ primary antibodies allowed me to monitor two of the pump proteins. Pump assembly was assed base on their localization within intracellular compartments. The pumps were mostly diffused within the cells at 1mg/ml (low) glucose (Figure 5A, C) using both anti- V_1A_1 and $V_1B_{1/2}$ primary antibodies, thus indicating a lower pump assembly. These results also indicate that the pumps are inactive as the V_1 domain remains detached from the V_0 domain. Pumps were specifically localized at 6mg/ml

high) glucose (Figure 5 B, D). These results indicate that the pumps are assembled and active when glucose levels are high.

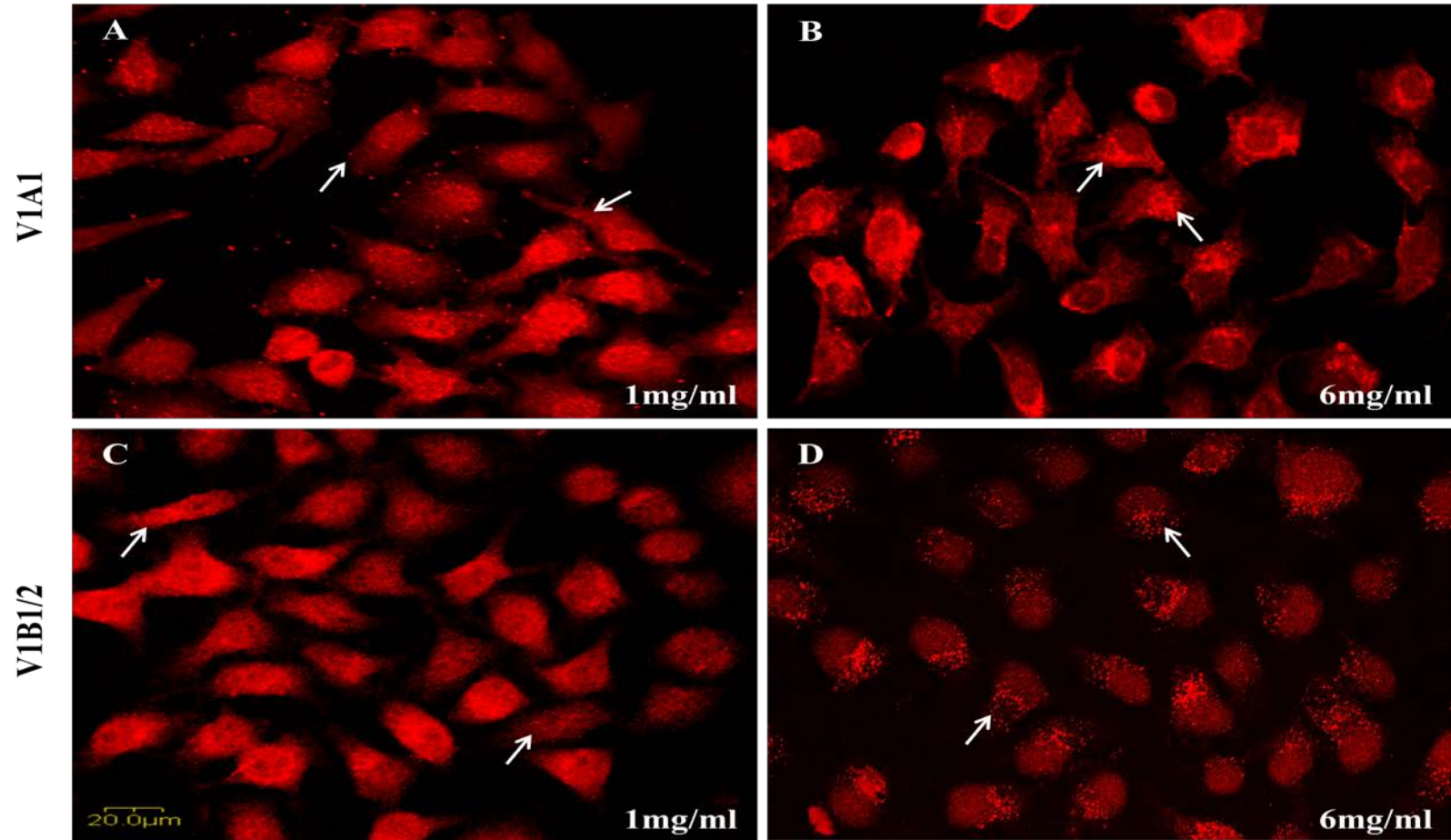


Figure 5. V-ATPase pump localization/assembly at low and high glucose concentrations. A, B, confocal imaging at 400x of V-ATPase pumps assembly/ localization at 1mg/ml and 6mg/ml of glucose in HeLa cells incubated with V₁A₁ primary antibody. C, D, images at 200x of the pumps assembly/localization at 1mg/ml and 6mg/ml of glucose incubated with V₁B_{1/2} primary antibody. Arrows indicate the V-ATPase pumps localization in a single cell; the pumps are represented with CY3 staining (red fluorescence).

Influenza viral infection is altered in response to changes in glucose concentration

Increasing extracellular glucose concentrations induces different levels of V-ATPase pump assembly in yeast (Kane 1995). We observed the same effect in HeLa cells with an increase in pump assembly at 6mg/ml glucose. To determine if this increased activity of the V-ATPase (which I determined to be specifically localized within intracellular compartments indicating higher activity) present with high glucose also leads to increased influenza replication, I examined influenza viral infection in MDCK cells grown at varying glucose concentrations (1, 2, 3, 4, and 6mg/ml) subsequently infected with influenza A H1N1. MDCK cells were used as they support the effective propagation and replication of many influenza type A and B viruses. Additionally, HeLa cells that were previously used could not be infected by influenza and my V₁A₁ and V₁B_{1/2} primary antibodies detect proteins only in human cells lines. Cells were immunostained with an anti-HA antibody to identify virally infected cells. Images were taken with a confocal microscope. Intensity of HA glycoprotein was visualized within cells. Positively infected cells were determined based on HA staining (CY3 red stains) specific to a cells (Figure 6). Higher intensity (staining) of HA glycoprotein within infected cells was observed at 4 and 6mg/ml (Figure 6 D, E) compared to 1, 2, and 3 mg/ml of glucose (Figure 6 A, B, C). Additionally, the percentage of infected cells was determined at each relative glucose level and increased as glucose concentration increased (Figure 7). The overall result from Figure 7 suggests that an increase in viral infection is associated with an increase in V-ATPase pumps activity/assembly when

extracellular glucose concentration is high. P-value = 0.028 when comparing viral infection at 1mg/ml and 6mg/ml glucose.

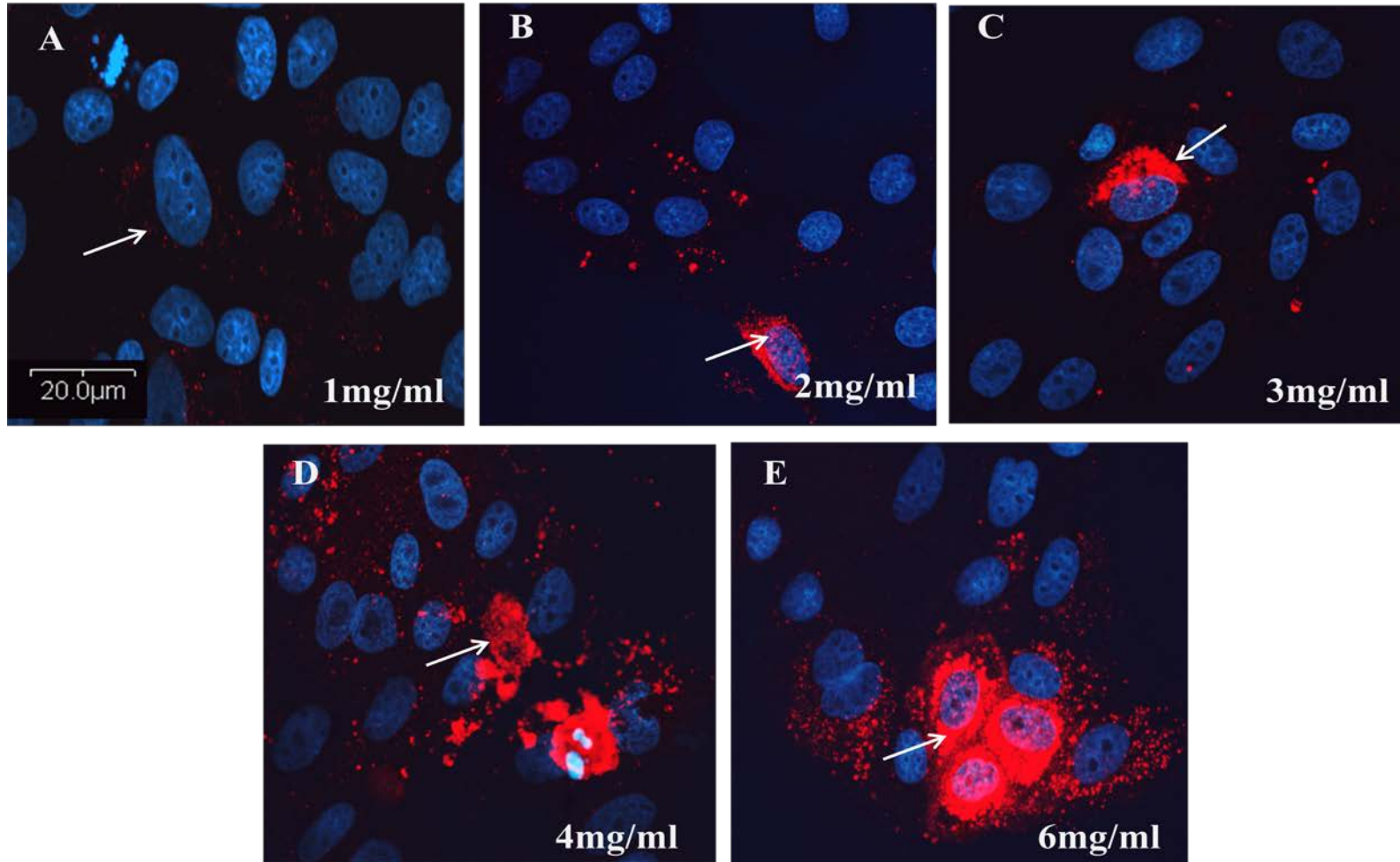


Figure 6. Increasing amounts of glucose increase influenza viral infection of MDCK cells. MDCK cells were infected with influenza A H1N1 for 24 hr. Cells were subsequently fixed and stained with anti-HA-antibody for the detection of viral particles. Blue stains represent the DNA of a single cell (DAPI) and CY3 (red staining) represent anti -HA antibody staining within infected cells. Confocal imaging was performed at 400x.

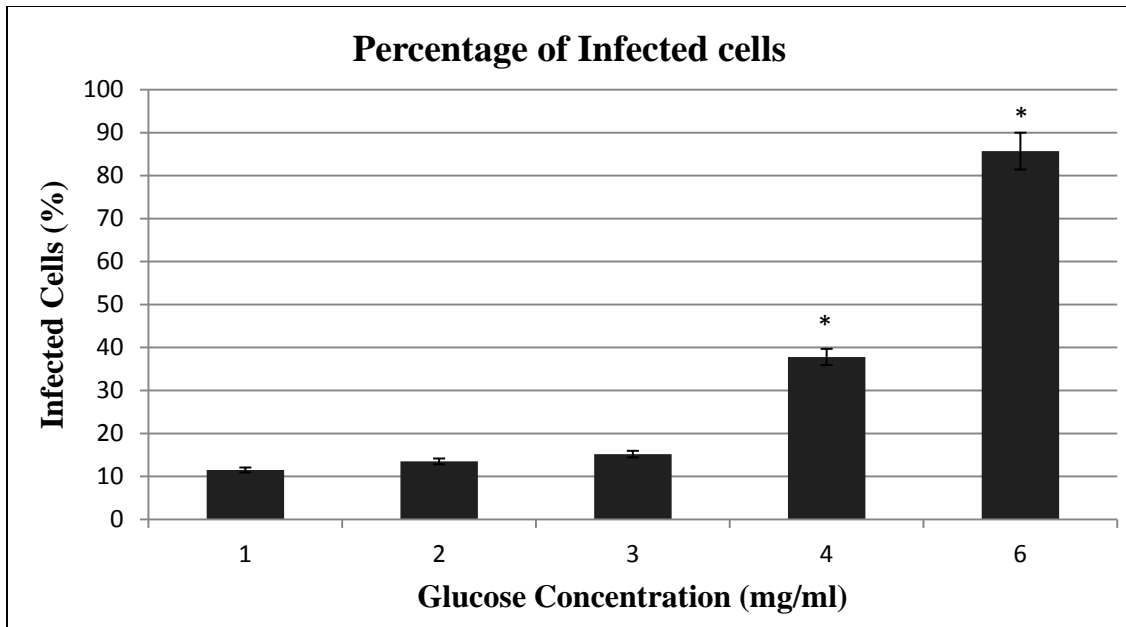


Figure 7. Graphical representation of the percentage of infected cells. Graph representing the percentage of infected cells at relative glucose levels. Percentage of infection increased as glucose levels increased. 1mg/ml (n=23), 2mg/ml (n=11), 3mg/ml (n=27), 4mg/ml (n=14), and 6mg/ml (n=12). Note: Numbers were provided as the percentage of infected cells in relation to the total number of cells per confocal image. * indicates a P-value ≤ 0.05 .

Increased glucose does not increase pump protein expression levels

To determine whether the increased pump localization that I saw with increased glucose was due to an increase in pump protein synthesis, I examined pump protein levels at varying glucose concentrations. HeLa cells were grown at 1, 2, 3, 4, and 6 mg/ml glucose, and the cellular proteins were separated by SDS-PAGE gel. HeLa were used since my V_1A_1 and $V_1B_{1/2}$ primary antibodies detect proteins only in human cell lines. Proteins were transferred to a nitrocellulose membrane and the protein levels were determined by western blot analysis using anti- V_1A_1 and $V_1B_{1/2}$ primary antibodies (Figure 8 A and B). As indicated in Figure 8 A and B, the protein of the 2 protein subunits did not increase with increased glucose, suggesting that increased protein localization was due to assembly, not additional protein synthesis.

The protein bands from varying glucose concentrations analyzed with V_1A_1 primary antibody were quantified with ChemiDoc software (Figure 9). With the results obtained, it is clear that there is not an increase of V-ATPase protein levels as I increased the glucose concentration.

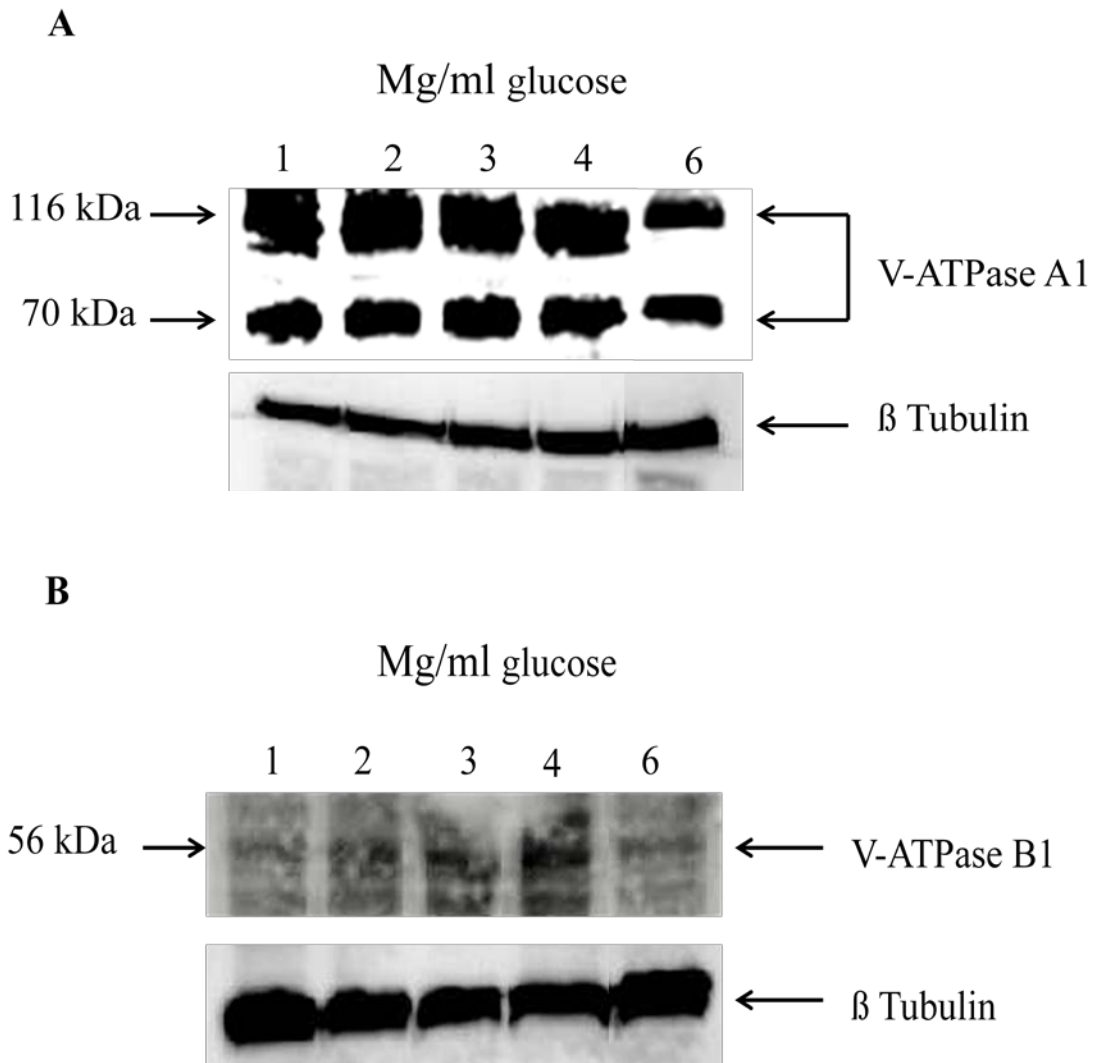


Figure 8. V-ATPase protein synthesis is not affected at varying glucose conditions. HeLa cells were grown at either 1, 2, 3, 4 and 6mg/ml of glucose. Western blot analysis was performed with an anti- V_1A_1 or anti- $V_1B_{1/2}$ antibody primary antibody. Band sizes were consistent for all glucose levels. Two isoforms of the A subunit are represented at 116kDa and 70kDa. B_1 subunit of the V-ATPase is located at 56kDa. Protein levels were standardized using tubulin protein levels.

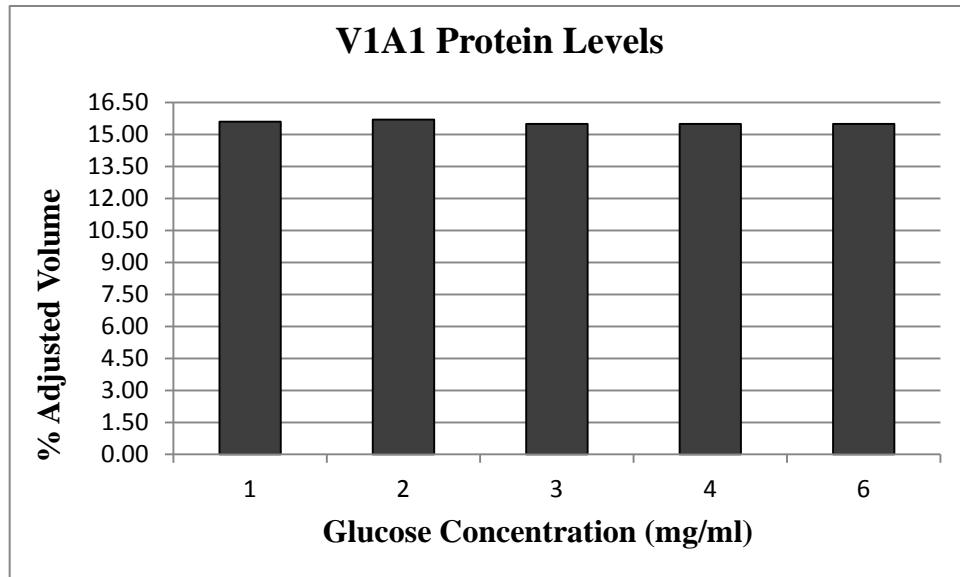


Figure 9. V-ATPase protein levels. Quantification of the V₁A₁ Western Blot products indicates that the V-ATPase protein synthesis remains constant for all glucose concentrations.

Inhibiting early glycolysis inhibits influenza viral infection

a) Glycolysis inhibition of hexokinase with 2-DG and 3-BrPa lowered influenza viral infection. Glycolysis inhibition with LND led to an increase in influenza

infection: Glucose metabolism was previously shown to affect the pumps assembly/disassembly (Parra & Kane 1998). ATP hydrolysis is needed to maintain pump assembly (Parra & Kane 1998). The pump disassembly was also attributed to a reduction in ATP levels (Para and Kane 1998). In this approach, I determined the effect of glycolytic inhibition on influenza infection. MDCK cells were treated for 24 hr with 2-DG, 3-BrPa and LND inhibitors of hexokinase, the first enzyme of the glycolytic pathway. 2-DG is an analogue of glucose and binds to hexokinase (thus inhibiting glucose phosphorylation by hexokinase) (Rui-hua Xu et al. 2005). 3-BrPa is an alkylating agent that inhibits hexokinase. LND is a molecule that inhibits glycolysis through inactivation of hexokinase. Immunostaining was conducted using an anti-HA antibody (Figure 10) and the percentage of infected cells was determined for each inhibitor treatment at their relative concentrations (Figure 11). The observed results indicate that 2-DG and 3-BrPa are effective inhibitors of influenza viral infection. Infection was lowered by 92.8% which was obtained by calculating the percent decrease of infected cells at 0mM and 5mM of 2-DG. Overall, a significant reduction in infected cells (P-value = 0.012) was observed when comparing the control treatment with 5mM of 2-DG. Additional, infection was reduced by 81.8% with 3-BrPa when comparing 0 μ M and 600 μ M of 3-BrPa (P-value = 0.035) (Figure 11 A, B). It is also important to note that

viral infection was not fully inhibited at 600 μ M of 3-BrPa. Unexpectedly, there was an increase in infection with LND treatment as I increased levels of the inhibitor (P-value = 0.05) (Figure 11 C). The obtained results were observed because LND reportedly enhanced glycolysis in normal cells, only causing a decrease in glycolysis in cancer cells (Floridi et al. 1981).

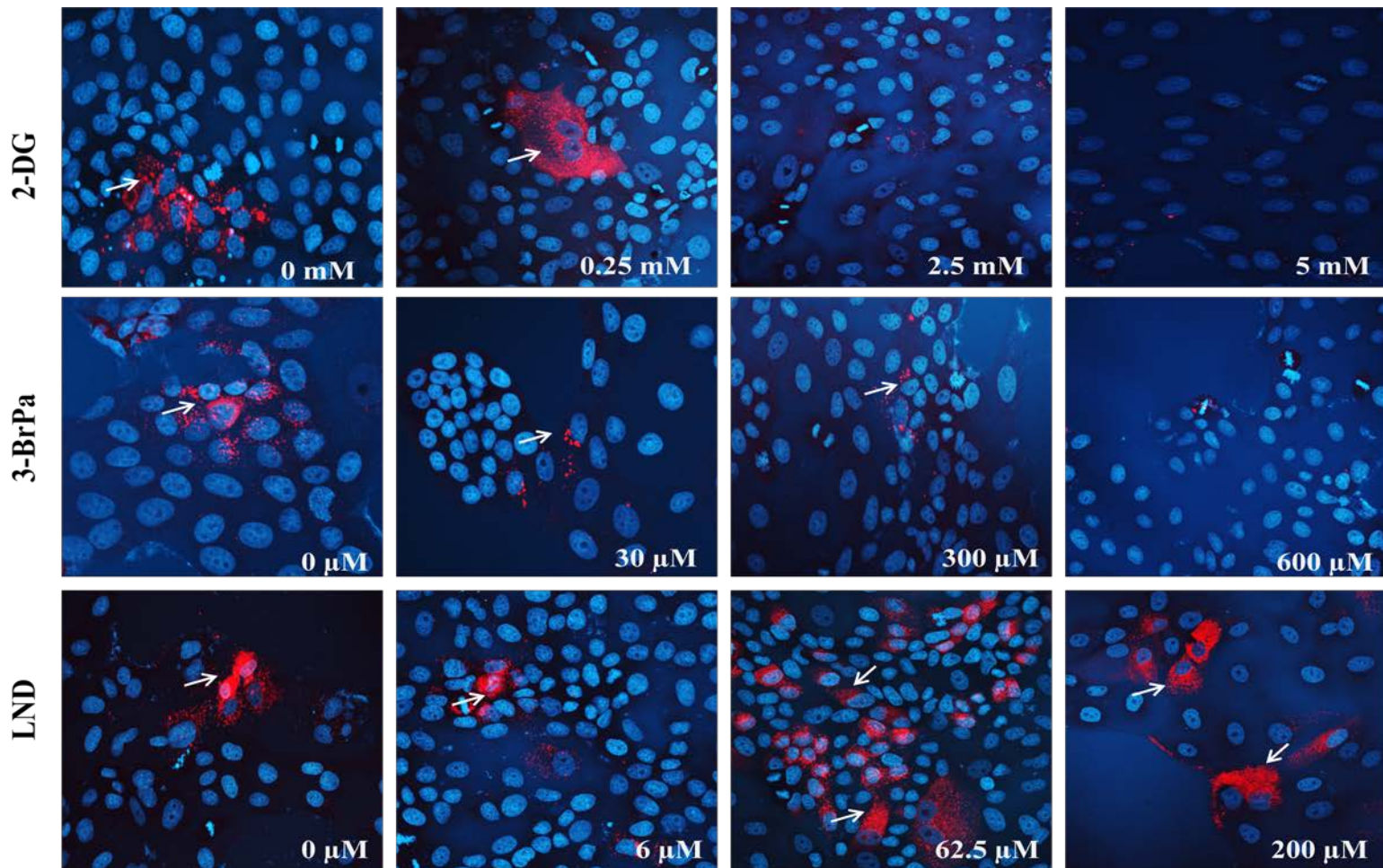


Figure 10. Confocal imaging of glycolytic pathway inhibition on influenza viral infection. MDCK cells were treated for 24hr with the glycolytic inhibitors 2-DG (0, 0.25, 2, 5mM), 3-BrPa (0, 30, 300, 600 μ M) and LND (0, 6, 62.5, 200 μ M,) and subsequently infected with influenza H1N1 for 24hr. Blue stains represent the DNA of a single cell (DAPI) and red staining (CY3) represent anti-HA antibody staining within infected cells. Arrows indicate infected cells after treatment with glycolytic inhibitors. Confocal imaging was performed at 400x at a scale of 20 μ M.

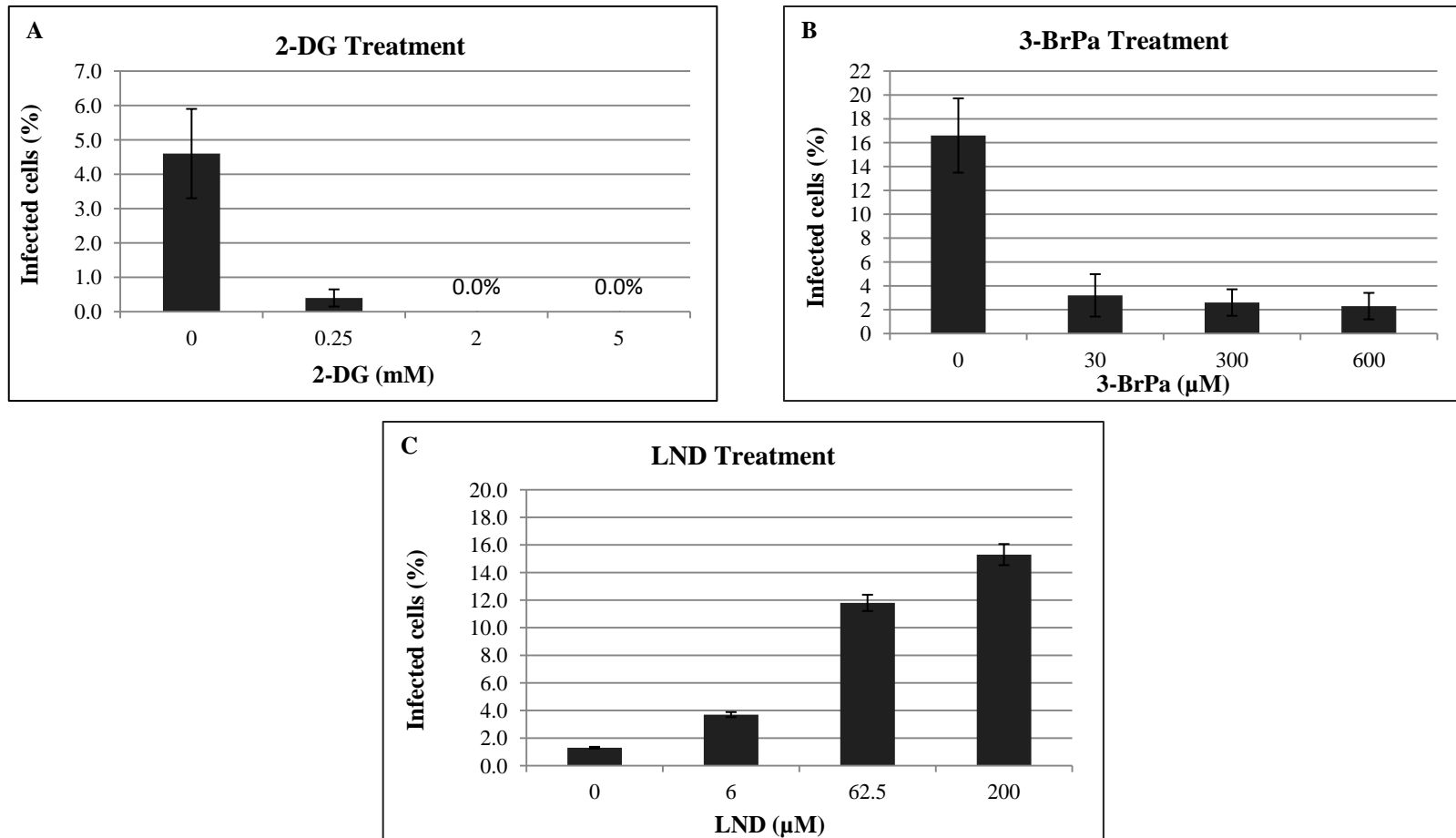


Figure 11. Percentage of infected cells after glycolytic inhibition. A, B, C, MDCK cells were treated for 24hr with the glycolytic inhibitors 2-DG (0, 0.25, 2, 5mM), 3-BrPa (0, 30, 300, 600μM) and LND (0, 6, 62.5, 200μM,) and subsequently infected with influenza H1N1 for 24hr. Cells were immunostained for determination of the percentage of infected cells. Number of infected cells for each concentration when compared to the control treatment had a P-value ≤ 0.05 .

b) Addition of extracellular ATP restored influenza viral infection: A further important approach that was conducted was to bypass glucose metabolism through addition of extracellular ATP and determine the subsequent influenza infection of cells. To accomplish this approach, 2-DG was used since my previous results indicate that infection was completely inhibited, compared to 3-BrPa, at the highest concentration used. Cells were first treated with the glycolytic inhibitor 2-DG (5mM) for 24hr. Influenza infection and ATP addition (50, 100 μ M) were conducted simultaneously. Immunostaining was performed with an anti-influenza protein (HA) antibody to detect infected cells. Viral infection remained unchanged at (-) ATP (Figure 12 A). 20.8% of infected cells was observed at 50 μ M ATP compared to (-) ATP with P-value = 0.004. A P-value of 0.006 was obtained when comparing (-) ATP to 100 μ M ATP treatment. The percentage of infected cells was relatively equal at 50 μ M and 100 μ M of ATP, and remained at 0% when ATP was not added (Figure 13).

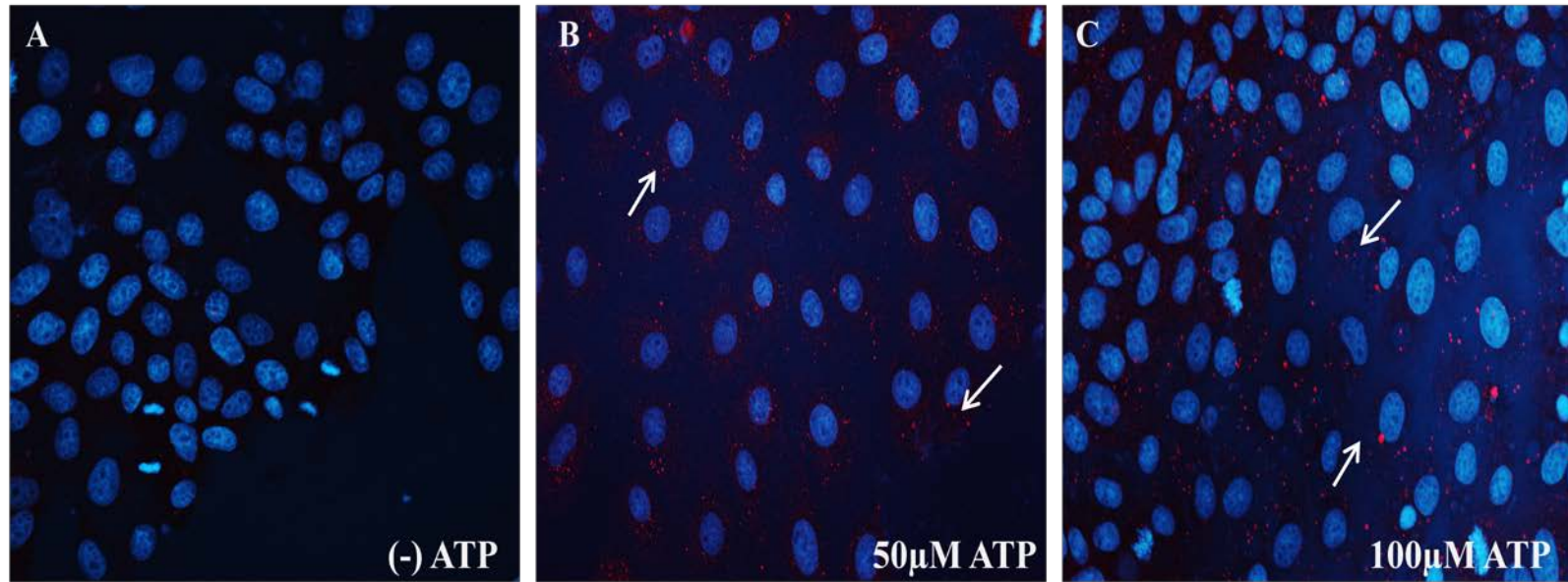


Figure 12. Effect of the addition of extracellular ATP. A, B, C, MDCK cells were treated for 24hr with the glycolytic inhibitor 2-DG (5mM) and subsequently infected with influenza A H1N1 for 24hr. ATP (50 μ M, 100 μ M) was added simultaneously. The control group was not treated with ATP after glycolytic inhibition. Arrows indicate HA protein of infected cells (CY3 red staining). DNA is stained in blue (DAPI). Confocal imaging was performed at 400x at a scale of 20 μ M.

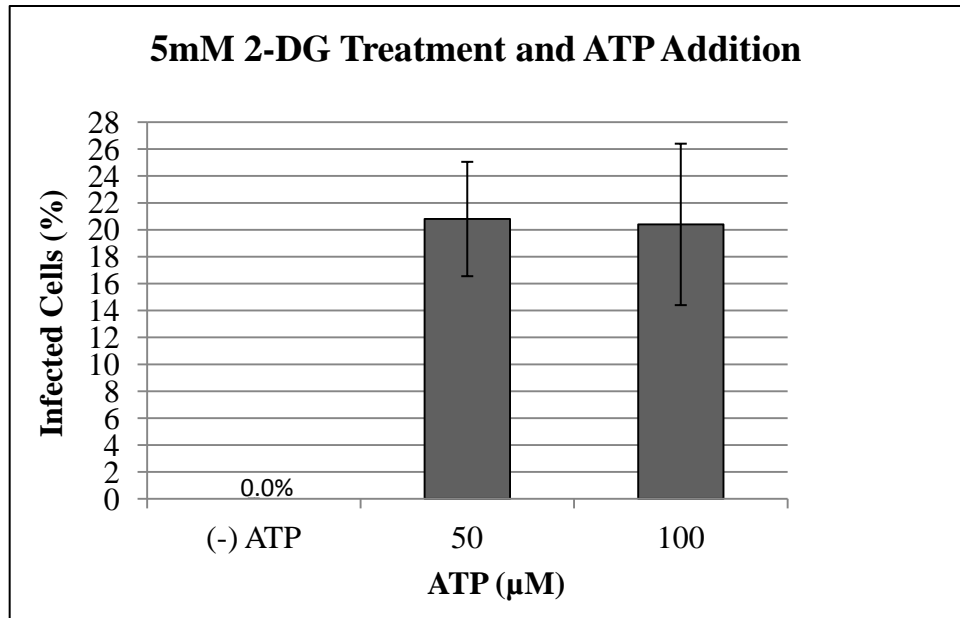


Figure 13. Percentage of infected cells after addition of extracellular ATP. Infection was restored 24hr post treatment with ATP with a P-value ≤ 0.05 comparing both ATP treatment group to the control (-) ATP. Percentage of infected cells were relatively equal at 50μM and 100μM of ATP (50μM = 20.8% and 100μM= 20.4%). (-)ATP n= 0, 50μM ATP n= 35, 100 μM ATP n= 82. Note: Percentages were determined relative to the total number of cells per confocal image. Note: Percentages were determined relative to the total number of cells per confocal image.

c) Inhibition of the pentose phosphate pathway lowered influenza infection: Cells were treated with 6-AN, an inhibitor of glucose-6-phosphate dehydrogenase, one of the rate limiting enzymes of the phosphate pentose pathway. This approach was conducted to determine alternative pathways the pumps may utilize to be active and initiate further infection. One potential pathway is the pentose phosphate pathway, which can generate intermediates of the glycolytic pathway such as fructose 6- phosphate and glyceraldehyde 3- phosphate depending on the cell need for energy. Both glycolytic intermediates can enter glycolysis and generate additional ATP that the V-ATPase pump can utilize and become active. This approach was conducted through immunostaining of MDCK cells to determine the percentage of infected cells (Figure 14) by confocal imaging. Inhibition of the pentose phosphate pathway lowered influenza viral replication by 100% at 250 μ M of 6-AN (Figure 14) when compared to the control, untreated cells (P-value = 0.018).

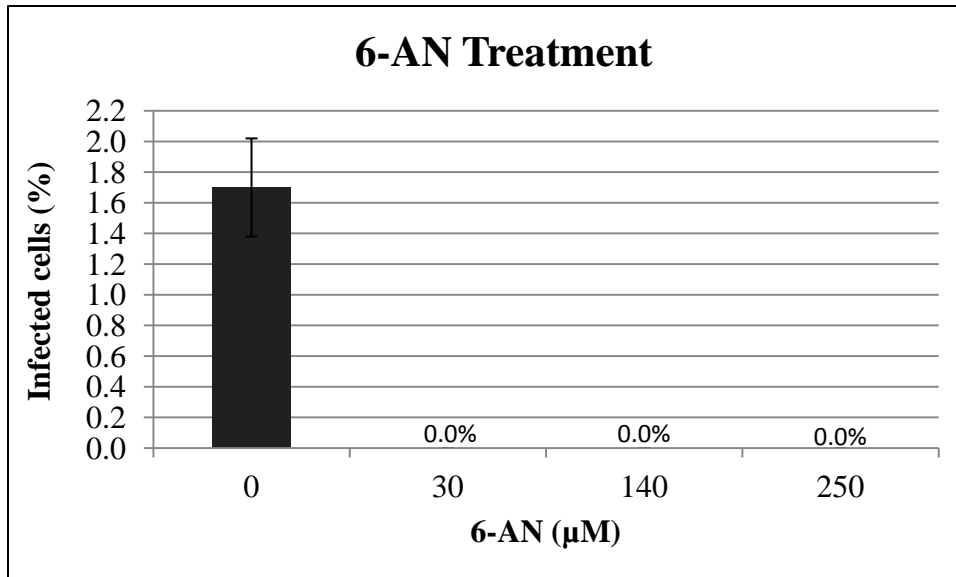


Figure 14. Percentage of infected cells after inhibition of the pentose phosphate pathway. Cells treated with the inhibitor of the pentose phosphate pathway 6-AN (0, 30, 140, 250µM) showed a decrease in infection when 6-AN concentration was increased. 0 µM n= 10, 30 µM n= 0, 140 µM n= 0 and 250 µM = 0.

CHAPTER IV

DISCUSSION

Influenza infection still remains a major public health concern. Most antiviral drugs target viral glycoproteins; thus, it is important to identify alternative ways to control influenza viral infection/replication by not only targeting viral particles but also by targeting the host cellular processes that the virus may utilize to induce infection. In this study, I targeted the activity of the V-ATPase proton pumps, which regulate the pH of intracellular compartments, in order to control influenza infection/replication.

In this report I demonstrated that regulating the V-ATPase pump activity via glucose metabolism can be a useful approach in controlling and inhibiting influenza infection in mammalian cells. As previously mentioned, the V-ATPase activity can be regulated through glucose depletion (Kane 2006) leading to disassembly of the V_1 and V_0 domains. Additionally, in yeast cells it was shown that the pump's assembly was modulated by the relative concentration of extracellular glucose (Para and Kane 1998). Comparing low (1mg/ml) and high (6mg/ml) extracellular glucose conditions in mammalian cells I provided additional evidence for a higher activity of the V-ATPase pumps at high glucose concentration (Figure 5 B, D), which is consistent with the fact that the pumps require ATP hydrolysis to be active. Thus, when more glucose molecules are metabolized to generate ATP, the pump's assembly is maintained or increased.

The higher HA intensity that was observed through visualization of HA staining within infected cells (CY3 red stain) at 4 and 6mg/ml glucose suggests that more glucose was available to initiate an increase in V-ATPase pump assembly/activity. The increase assembly/activity of the pump then led to an increase in virally infected cells (Figure 7).

Western blot analysis confirmed that the increased pump localization was not due to increased pump subunit synthesis. These results indicate that while higher glucose levels lead to an increased assembly of the pumps, the relative protein synthesis of the V-ATPase pumps is not associated with higher amount of glucose concentrations (Figure 8, 9).

To find an inhibitor of the V-ATPase activity that would inhibit viral infection, I focused on the glycolytic pathway. Glycolysis is the process by which glucose metabolism occurs to generate a net gain of two ATP, two NADH⁺ and two molecules of pyruvate (Pelicano et al 2006). I analyzed glycolytic inhibition of the hexokinase enzyme with 2-DG, 3-BrPa and LND. Hexokinase is one of the key enzymes of the glycolytic pathway. Hexokinase specifically phosphorylates glucose molecule to create glucose-6-phosphate (G-6P). This activity traps G-6P in the cells and serves as the starting point for glucose to enter glycolysis (Peliciano et al. 2006). Thus, by inhibiting hexokinase I prevented the initial metabolism of glucose. 2-DG is an analogue of glucose that is capable of binding to hexokinase (thus inhibiting glucose phosphorylation by hexokinase) (Rui-hua Xu et al. 2005). 3-BrPa is an alkylating agent that inhibits hexokinase. LND is a molecule that inhibits glycolysis through inactivation of hexokinase. Additionally, both 3-BrPa and LND can affect oxidative phosphorylation (Hulleman et al. 2009). I showed

that inhibition of the glycolytic pathway for 24hr with 2-DG and 3-BrPa specifically reduced influenza infection compared to cells that were not treated with the inhibitors. Thus, the intracellular ATP level was lowered, leading to a decrease in the pump activity which is also consistent with the pumps needing energy to properly function and help induce infection. A 92.8% decrease in infection was observed with the 5mM 2-DG treatment and a reduction of 81.8% with the 600 μ M 3-BrPa treatment when compared to the control group. It is important to note that infection was not completely inhibited at 600 μ M 3-BrPa. Higher 3-BrPa concentrations may be required for complete inhibition of influenza infection. While infection was inhibited with 2-DG and 3-BrPa, inhibition of hexokinase with LND significantly increased influenza infection in MDCK cells. The relevant results were observed because LND reportedly enhances glycolysis in normal cells, only causing a decrease in glycolysis in cancer cells (Floridi et al. 1981). Additional information about this preference in activity by LND is scarce. However, this selection in activity may be due to the mitochondrially bound hexokinase which is usually absent in normal cells (Floridi et al. 1981).

ATP is considered to activate the V-ATPase pumps by binding to its catalytic site on the A and B subunits of the pump. In the present study, I bypassed glucose metabolism through the addition of extracellular ATP after inhibition of glycolysis. Addition of extracellular ATP after glycolytic inhibition with 2-DG (5mM) restored influenza infection in mammalian culture cells, presumably through reassembly of the V_1 and V_0 domains. This suggests that glycolysis is not actually required to take place in order to activate the pump. With the results obtained in this study, the presence of ATP

may be considered the principal activator of the pumps, and not necessarily the interaction of glycolytic enzymes with the V-ATPase pump.

Another major approach of my study was to identify an alternative pathway the virus may utilize to induce infection. I inhibited glucose 6-phosphate dehydrogenase, a rate limiting enzyme of the pentose phosphate pathway, using 6-AN. The pentose phosphate pathway uses sugar to synthesize ribose 5-phosphate in nucleotides or nicotinamide adenine dinucleotide phosphate-oxidase (NADPH) production (Delvin M.T 2011). This pathway provides a mean of converting ribose 5-phosphate to form intermediates of the glycolytic pathway such as fructose 6-phosphate (F6P) and glyceraldehydes 3-phosphate (G3P). Both F6P and G3P can enter glycolysis for additional ATP synthesis. I found that inhibiting the pentose phosphate pathway caused a decrease in influenza viral infection. These findings suggest that generation of additional ATP through the pentose phosphate pathway may be an alternative way the pumps may utilize to be active when hexokinase, the first enzyme of glycolysis, is inhibited. Thus, 6-AN can lead to ATP depletion by also interfering with glucose metabolism through inhibiting the production of intermediates of the glycolytic pathway. Since the rate limiting enzyme of the pentose phosphate was inhibited, not only intermediates of the glycolytic pathway but also NADPH production were inhibited. Thus, it may be suggested that NADPH is also necessary for viral infection. Further studies will need to be conducted to determine if NADPH has a direct effect on V-ATPase activity or directly affects viral infection. A model of V-ATPase pump activity and influenza infection is presented in Figure 15.

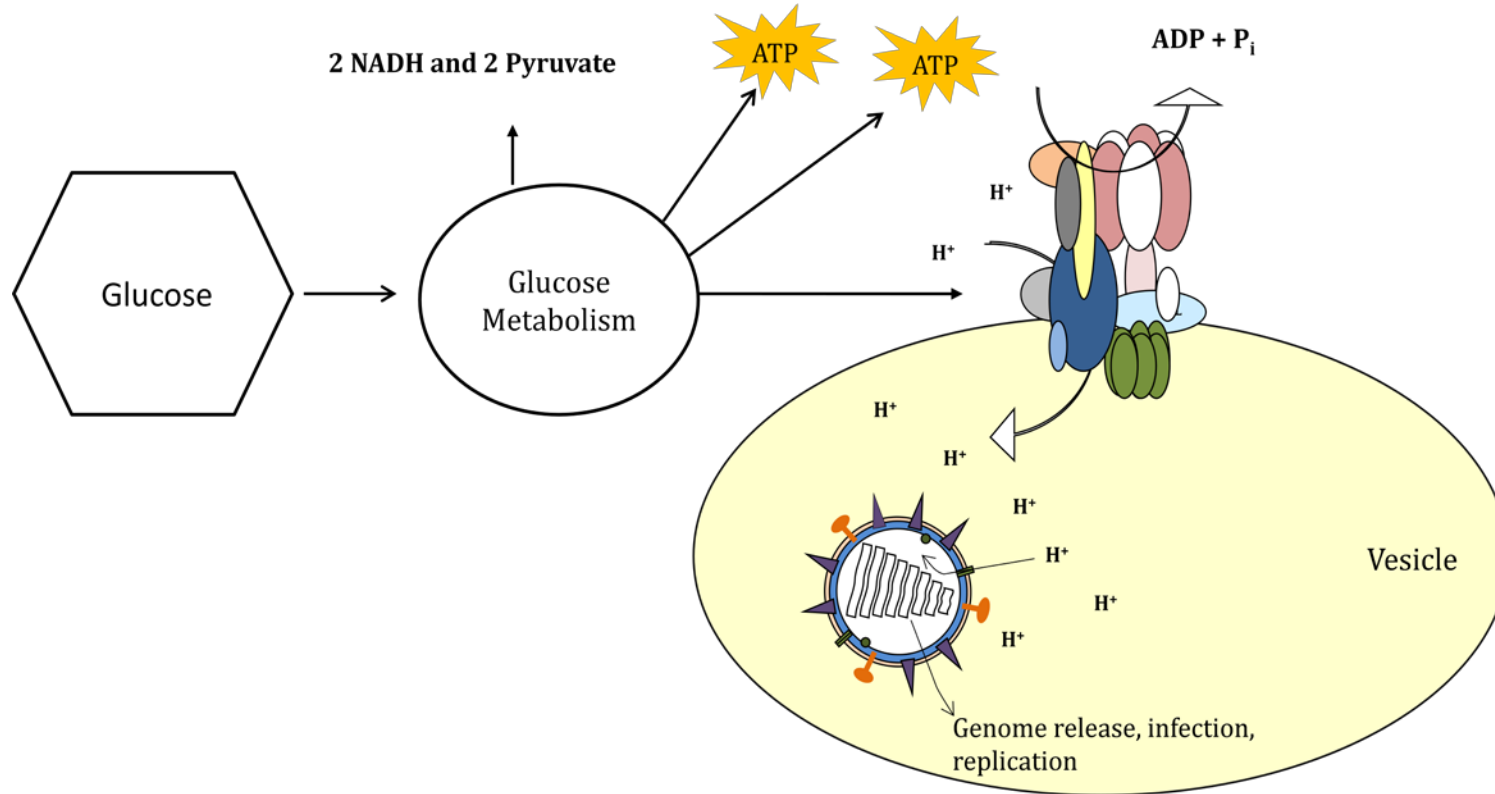


Figure 15. Schematic representation of glucose metabolism on V-ATPase activation and influenza viral infection. ATP activates the V-ATPase pump by binding to its catalytic site, and protons are transported against the gradient into the vesicle. The acidic environment of the vesicle initiates activation of the M2 ion channel leading to proton transport into the viron and subsequent release of viral genome into the cytosol. (Modified from Lu M. , Sautin Y. et al. 2004).

REFERENCES

1. BERENS GEORG, GOOTSCHALK RENE et al., 2006 Pathogenesis and Immunology., pp 92-105 in Influenza Report, edited by KAMPS B. S., HOOFMANN C. and PREISER W., Flying Publisher, Paris, Cagliari, Wuppertal and Sevilla.
2. BETAKOVA T. (2007) M2 protein- A proton channel of influenza A virus. *Current Pharmaceutical Design* **13**: 3231-3235.
3. BEYENBACH KLAUS and WIECZORECK HELMUT, 2005 The V-ATPase: molecular structure and function, physiological roles and regulation. *J ExpBiol* **209**: 577-589.
4. BOND S., FORGAC M., 2008 The Ras/Camp/protein kinase A pathway regulates glucose-dependent assembly of the vacuolar (H⁺)-ATPase in yeast. *J Biol Chem.* **283**: 36513-36521.
5. BUDIHardjo I.I., WALKKER D.L and SVINGEN P.A, 1998 6-Aminonicotinamide sensitizes human tumor cell lines to cisplatin. *Clin. Cancer Res.* **4**:117-130.
6. CHATTERJEE, D., CHAKRABORTY, M., LEIT, M. *et al* 1992 The osteoclast proton pump differs in its pharmacology and catalytic subunits from other vacuolar H⁺ATPases. *J. ExpBiol* **172**: 193-204.
7. DEVLIN THOMAS (2011) Pentose Phosphate Pathway., pp 648-652 *Textbook Biochemistry with Clinical Correlations*, edited by DEVLIN THOMAS, John Wiley & Sons Inc., Hoboken, NJ.
8. FLORIDI ARISTIDE, PAGGI G. MARCO *et al* 1981. Lonidamine a selective inhibitor of aerobic glycolysis of murine Tumor Cells. *JNCI* **66**.
9. GUINEA, R., and L. CARRASCO, 1995 Requirement for vacuolar proton-ATPase activity during entry of influenza virus into cells. *J. Virol.* **69**: 2306-2312.
10. HARVEY, W. R., 1992 Physiology of V-ATPases. *J. exp. Biol.* **172**: 1-17.

11. HIRATA T., IWAMATO-KIHARA A. *et al.*, 2003 Subunit rotation of vacuolar type proton pumping ATPase: relative rotation of the G and C subunits. *J BiolChem* **279**: 23714-23719.
12. HULLEMAN E., KAZEMIER K.M, *et al.* 2009 Inhibition of glycolysis modulated prednisolone resistance in acute lymphoblastic leukemia cells. *Blood Journal*. **113**: 2014-2021.
13. JEFFERIES, K.C, D.J, *et al.* 2008 Function, structure, and regulation of the vacuolar (H⁺)-ATPases. *Arch Biochem.Biophys.***476**: 33-42.
14. KANE P. M., 1995 Disassembly and reassembly of the yeast vacuolar H⁺ ATPase in vivo. *J. BiolChem* **270**:17025-17032.
15. KANE P. M., 2006 The where, when and how of organelles acidification by the yeast vacuolar H⁺-ATPase. *Micro & MolBiol Rev.* **70**: 177-191.
16. KAKINUM Y., OHSUMI Y. and ANRAKU Y.,1981 Properties of H⁺-translocating adenosine triphosphatase in vacuolar membranes of *Saccharomyces cerevisiae*. *J. BiolChem* **256**:10859-10863.
17. KLEIN, U., 1992 The insect V-ATPase, a plasma membrane proton pump energizing secondary active transport: immunological evidence for the occurrence of a V-ATPase in insect ion transport in epithelia. *J. exp. Biol.* **172**: 345-354.
18. LU M., SAUTIN YY, *et al.*, 2004 The glycolytic enzyme aldolase mediates assembly, expression and activity of vacuolar H⁺ATPase. *J Biol Chem.* **279**: 8732-8739.
19. LU M., HOLLIDAY LS *et al.*, 2001 Interaction between aldolase and vacuolar H⁺-ATPase: evidence for direct coupling of glycolysis to the ATP- hydrolyzing proton pump. *J BiolChem* **276**: 30407-13.
20. NISHI T., FORGAC M., 2002 The vacuolar H⁺-ATPase: Nature's most versatile proton pumps. *Nat Rev Mol Cell Biol.* **3**: 94-103.
21. PALESE P., and M.L. SHAW, 2007 Orthomyxoviridae: The virus and the replication., pp 1647-1732 in *Fields Virology*, edited by D.M. KNIPE and P.M. HOWLEY, Lippincott, Williams, & Wilkins, Philadelphia, PA.

22. PARRA K. J, KANE P.M., 1998 Reversible association between the V₁ and V₀ domains of yeast vacuolar H⁺-ATPase is an unconventional glucose-induced effect. *Mol Cell Biol.* **18**: 7064-7074.
23. PELICANO H., MARTIN DS, XU R-U and HUANG P., 2006 Glycolysis inhibition for anticancer treatment. *Oncogene* **25**: 4633-4646.
24. PROBST I. QUENTMEIER A. *et al.*, 1988/1989 Stimulation by insulin of glycolysis in cultured hepatocytes is attenuated by extracellular ATP and puromycin through purine-dependent inhibition of phosphofructokinase 2 activation. *Eur. J. Biochem.* **182**: 387-393.
25. SU Y., ZHOU A, *et al.*, 2003 The a subunit of the V-type H⁺ ATPase interacts with phosphofructokinase 1 in humans. *J Biol Chem.* **278**: 20013-8.
26. SZE HEVEN, SCHUMACHER KARIN *et al.*, 2002 A simple nomenclature for a complex proton pump: VHA genes encode the Vacuolar H⁺ ATPase. *Trends in Plant Sci.* **7**: 157-161.
27. WAGNER CA, FINBERG KE *et al.*, 2004 Renal vacuolar H⁺-ATPase. *Physiol Rev.* **84**:1263-314.
28. XU RUI-HUA *et al.*, 2005 Inhibition of Glycolysis in cancer cells: A novel strategy to overcome drug resistance associated with mitochondrial respiration Defect and Hypoxia. *Cancer Res.* 65 (2): 613-621.
29. XU TING and FORGAC M., 2001. Microtubules are involved in glucose dependent dissociation of the yeast vacuolar H⁺-ATPase in vivo. *J Biol Physiology.* **276**: 24855-24861.